Efficient Radical-Based NIR Organic Light-Emitting Diodes with Emission peak Exceeding 800 nm

Kuo Lv, Ming Zhang and Feng Li*

State Key Laboratory of Supramolecular Structure and Materials, College of Chemistry, Jilin University Changchun, 130012, P. R. China

*E-mail: lifeng01@jlu.edu.cn

Contents

General information

All reagents and solvents required for synthesis and characterization are purchased from commercial suppliers and used directly without any treatment. The nuclear magnetic resonance (^{1}H NMR) spectra were recorded on the Bruker AVANCEIII 500 spectrometer at 500 MHz at 298 K and tetramethyl silane (TMS) (δH = 0 ppm) as the internal standard. MALDI-TOF mass spectra were recorded on a Brucker Autoflex speed TOF/TOF mass spectrometer with DCTB as a matrix. A shimadzu UV-2550 spectrophotometer was applied to record the ultraviolet (UV)-visible spectra. Fluorescence spectra were recorded using a RF-5301 PC spectrophotometer and QE pro. All of PLQEs are determined with a calibrated integrating sphere system and using QE pro of Ocean Insight as fluorescence spectrometer. The electrochemical oxidation and reduction potentials were recorded using an electrochemical analyzer (CHI660C, CH Instruments, USA). The fluorescence decay spectra were recorded on an Edinburgh fluorescence spectrometer (FLS980), and the lifetime of the excited states was measured by the time-correlated single photon counting method under the excitation of a laser (378 nm). Elemental analysis (C, H and N) was performed on a Elementar Vario micro cube elemental analyzer. Thermal gravimetric analysis (TGA) was characterized by a TAINSTRUMENTS Q500 TGA analyzer. Ready-made indium tin oxide (ITO) glass substrates were purchased and cleaned. After dried with N2, they were treated with UV irradiation for 20 min and next transferred to a vacuum deposition system with the pressure of 1-4×10^{-6} mbar. The MoO_3 layer was deposited at a rate of 0.1 Å s^{-1}. All the organic layers were deposited at 0.2-0.4 Å s^{-1}. The evaporation rate of cathode LiF

and Al metal layer were 0.1 Å s^{-1} and 0.3-0.8 Å s^{-1} respectively. The current-voltage characteristics were measured using a Keithley 2400 programmable electrometer. The EL spectra and EQEs were measured using QE pro spectroradiometer of Ocean Insight together with a calibrated integrating sphere at room temperature in glove box.

1. Synthesis Section

The HTTM was prepared as reported[1].

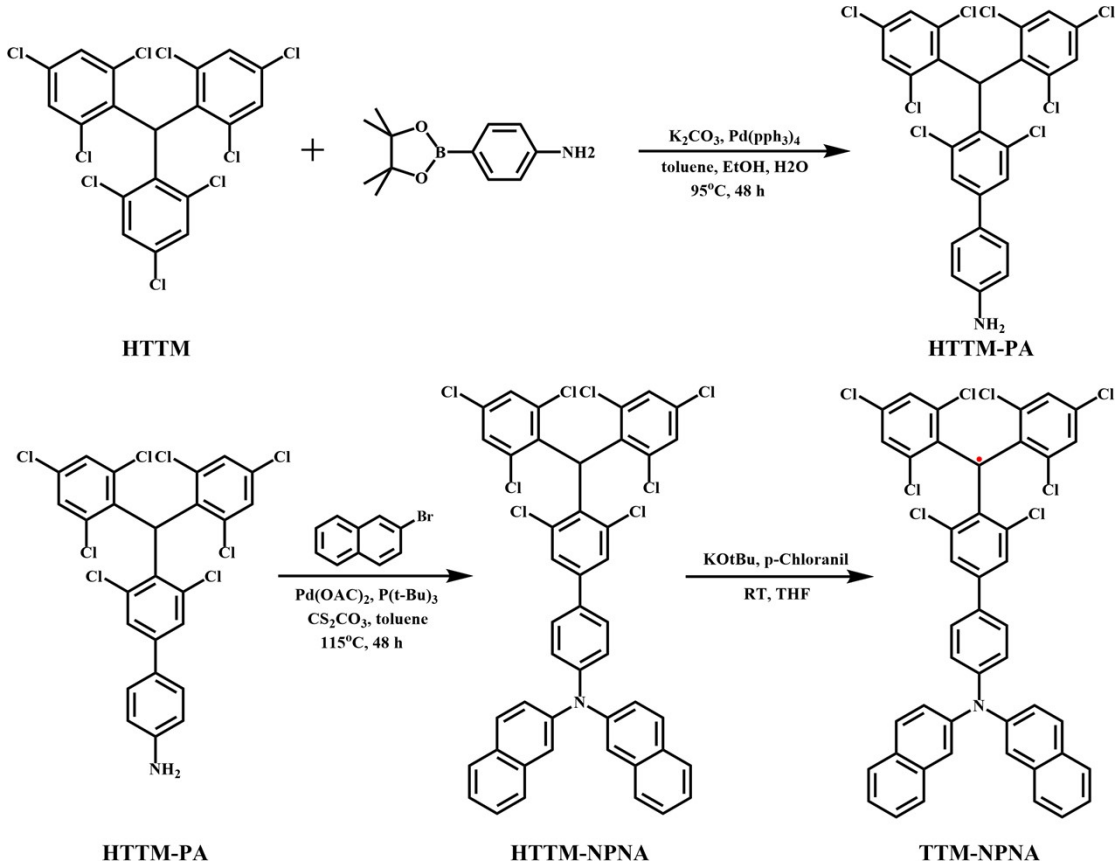

Scheme S1. The synthesis route of **TTM-NPNA**

(1) Synthesis of **HTTM-PA**

HTTM (1.00 g, 1.80 mmol) and 4-(4,4,5,5-tetramethyl-1,3,2-dioxaborolan-2-yl) - aniline (0.39 g, 1.80 mmol) was dissolved in a mixed solvent of toluene (12 ml), K_3PO_4 aqueous solution (8 ml, 2 mol / L) and ethanol (4 ml), and catalyst $Pd(PPh_3)_4$ (0.10 g, 0.09 mmol) was added under argon atmosphere. The mixture was stirred at 95℃ for 48

h under argon atmosphere. After the reaction mixture cooling to room temperature, the solution was extracted with dichloromethane. Organic layer was collected and dried. The solvent was removed under vacuum and the crude product was purified by silica gel column chromatography (using petroleum ether: dichloromethane = 8:1 v/v). **HTTM-PA** was obtained as a white solid (0.39 g, 36% yield). ^{1}H NMR (500 MHz, CD_2Cl_2) δ 7.54 (d, J = 2.0 Hz, 1H), 7.41 (s, 2H), 7.41 – 7.40 (m, 2H), 7.39 (s, 1H), 7.29 – 7.25 (m, 2H), 6.76 (s, 1H), 6.75 (d, J = 3.7 Hz, 2H), 4.08 (s, 2H). MALDI-TOF-MS (m/z): calculated for $C_{25}H_{13}Cl_8N$, 608.853; found, 608.664. Elem. Anal. Calcd for $C_{25}H_{13}Cl_8N$: C 49.15, H 2.14, N 2.29; found, C 50.11, H 2.43, N 2.29.

(2) Preparation of **HTTM-NPNA**

HTTM-PA (1.22 g, 2.00 mmol) and 2-bromonaphthalene (1.24 g, 6.00 mmol) was dissolved in dry toluene (25 ml). Pt(t-Bu)$_3$ (0.62 ml, 10%w/v, 0.30 mmol), Cs_2CO_3 (1.95 g, 6.00 mmol) and catalyst Pd(OAc)$_2$ (33.70 mg, 0.15 mmol) was added under argon atmosphere. The mixture was stirred at 115°C for 48 h under argon atmosphere. After the reaction mixture cooling to room temperature, the solution was extracted with dichloromethane. Organic layer was collected and dried. The solvent was removed under vacuum and the crude product was purified by silica gel column chromatography (using petroleum ether: dichloromethane = 10:1 v/v). **HTTM-NPNA** was obtained as a white solid (1.02 g, 59% yield). ^{1}H NMR (500 MHz, CD_2Cl_2) δ 7.84 (s, 1H), 7.82 (d, J = 2.7 Hz, 2H), 7.81 (d, J = 2.4 Hz, 1H), 7.66 (d, J = 2.1 Hz, 1H), 7.65 (s, 1H), 7.54 (s, 2H), 7.44 (d, J = 1.9 Hz, 1H), 7.43 (s, 2H), 7.42 (d, J = 2.1 Hz, 2H), 7.38 (d, J = 2.2 Hz, 1H), 7.34 (d, J = 2.2 Hz, 1H), 7.32 (d, J = 2.2 Hz, 2H), 7.24 (d, J = 2.2 Hz, 1H), 7.07

(d, J = 2.4 Hz, 1H), 6.93 (d, J = 2.4 Hz, 1H), 6.71 (s, 1H). MALDI-TOF-MS (m/z): calculated for $C_{45}H_{25}Cl_8N$, 862.944; found, 862.063. Elem. Anal. Calcd for $C_{45}H_{25}Cl_8N$: C 62.61, H 2.92, N 1.62; found, C 62.65, H 2.80, N 1.63.

(3) Preparation of **TTM-NPNA**

Under argon atmosphere and in the dark, **HTTM-NPNA** (0.86 g, 1.00 mmol) was dissolved in dry THF (20 ml). Then t-BuOK (1.12 g, 10.00 mmol) was added. The solution was stirred for 5 h in the dark at room temperature, and then p-Chloranil (1.23 g, 5.00 mmol) was added. The solution was stirred for further 1 h. After the reaction finished, the solvent was removed under vacuum and the crude product was purified by silica gel column chromatography (using petroleum ether: dichloromethane = 10:1 v/v). The crude product was recrystallized twice from dichloromethane and methanol and a gray solid was obtained (0.65 g, 75% yield). MALDI-TOF-MS (m/z): calculated for $C_{45}H_{24}Cl_8N$, 861.936; found, 861.064. Elem. Anal. Calcd for $C_{45}H_{24}Cl_8N$: C 62.68, H 2.81, N 1.62; found, C 62.80, H 2.92, N 1.58.

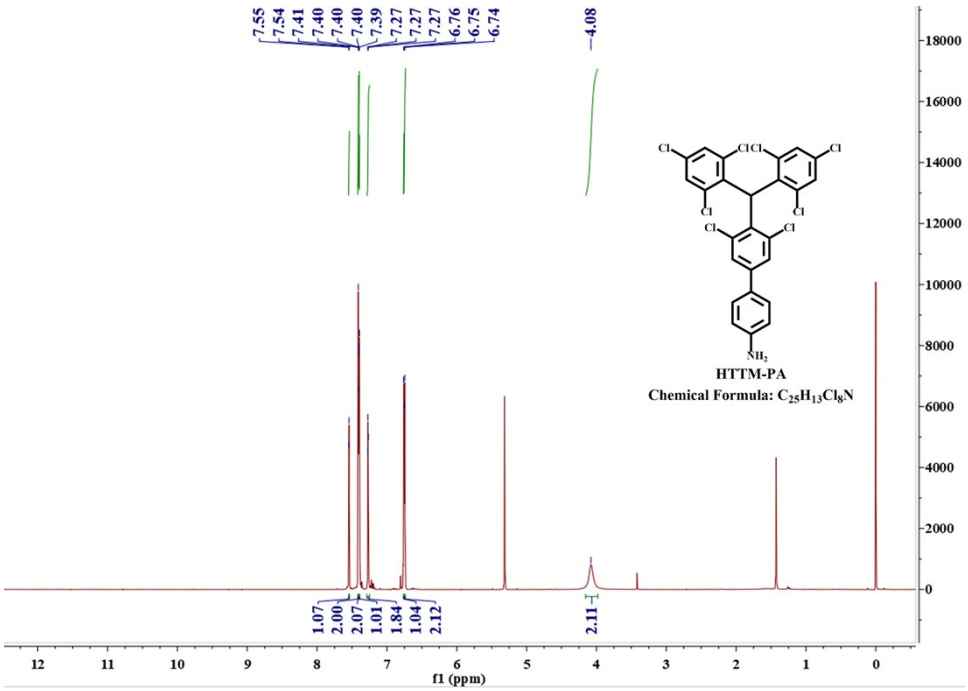

Fig. S1 ^{1}H-NMR spectrum of **HTTM-PA** in CD_2Cl_2.

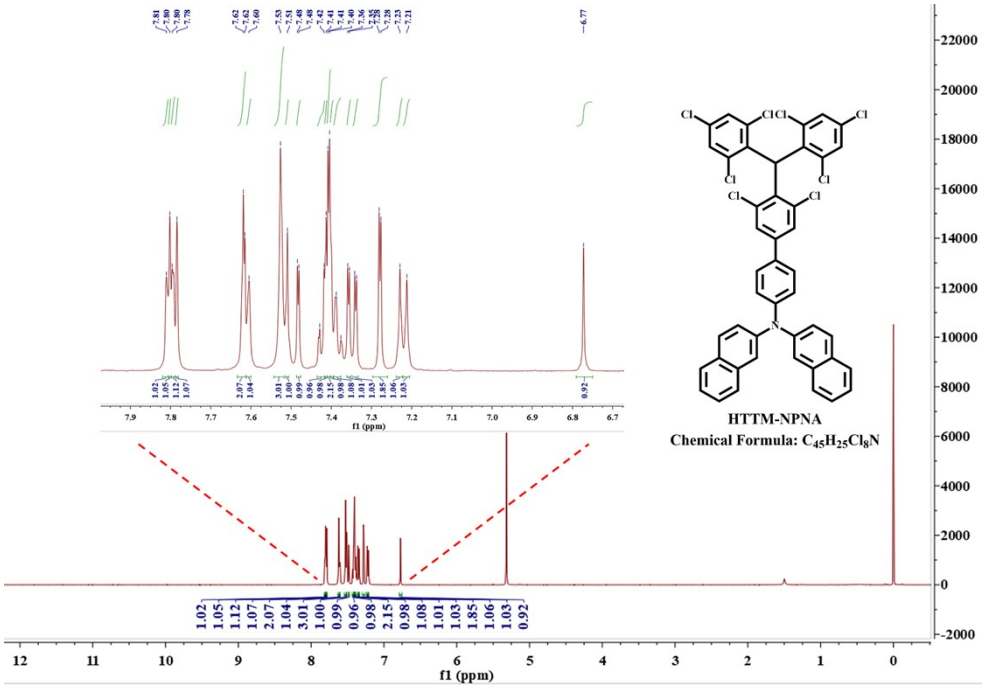

Fig. S2 ^{1}H-NMR spectrum of **HTTM-NPNA** in CD_2Cl_2.

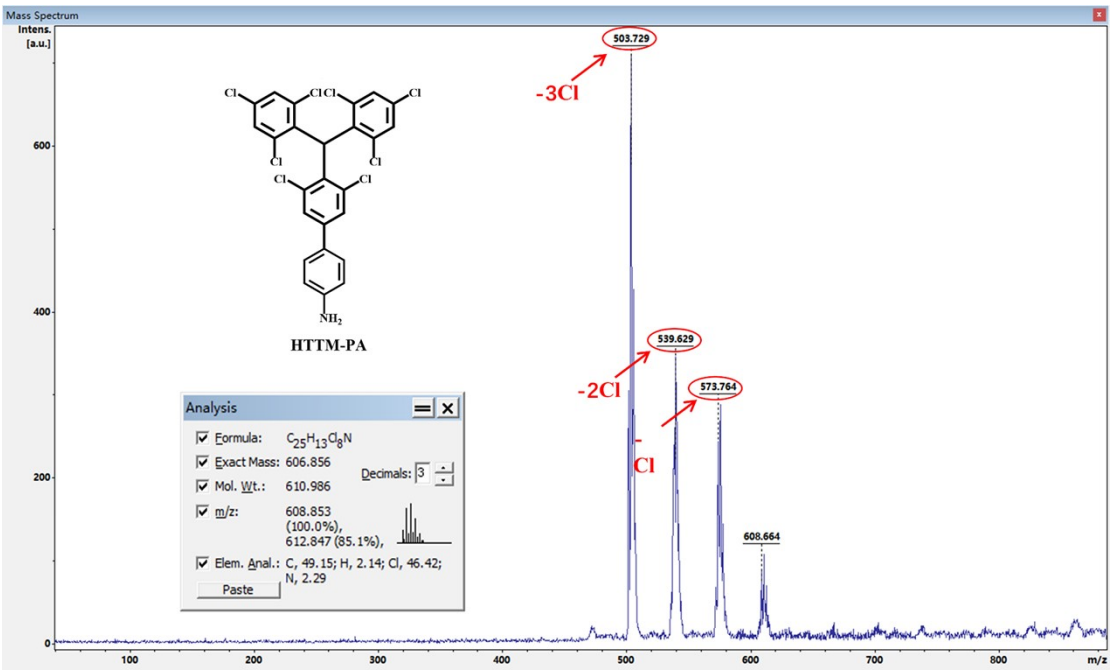

Fig. S3 MALDI-TOF-MS spectrum of **HTTM-PA**.

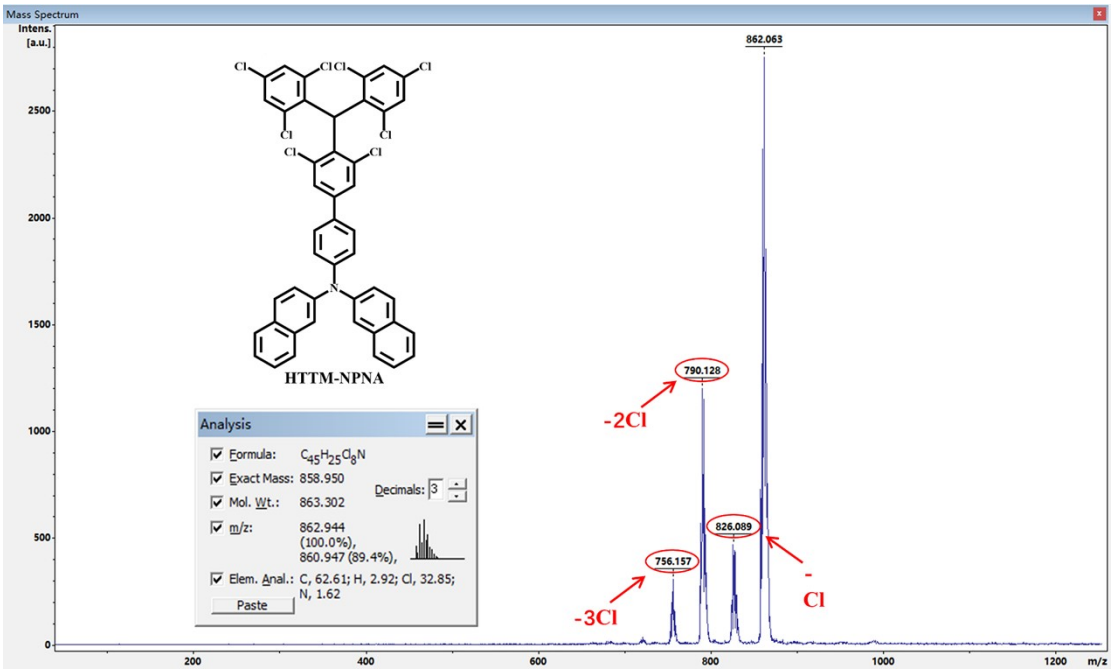

Fig. S4 MALDI-TOF-MS spectrum of **HTTM-NPNA**.

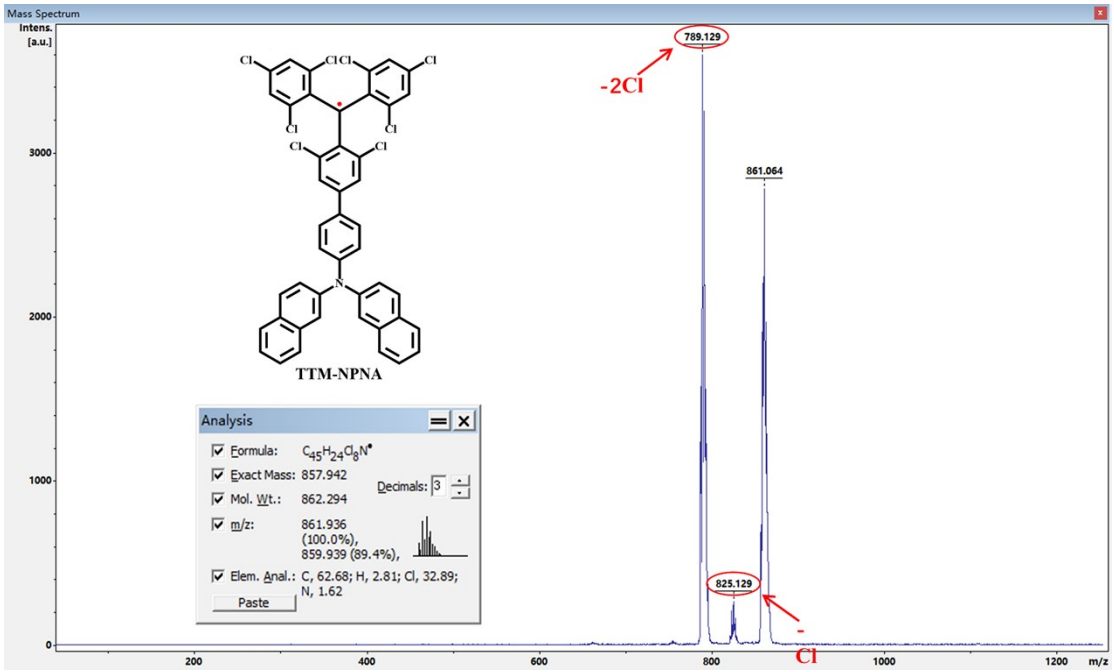

Fig. S5 MALDI-TOF-MS spectrum of **TTM-NPNA**.

2.Photophysical Parameters of TTM-NPNA in different solvents

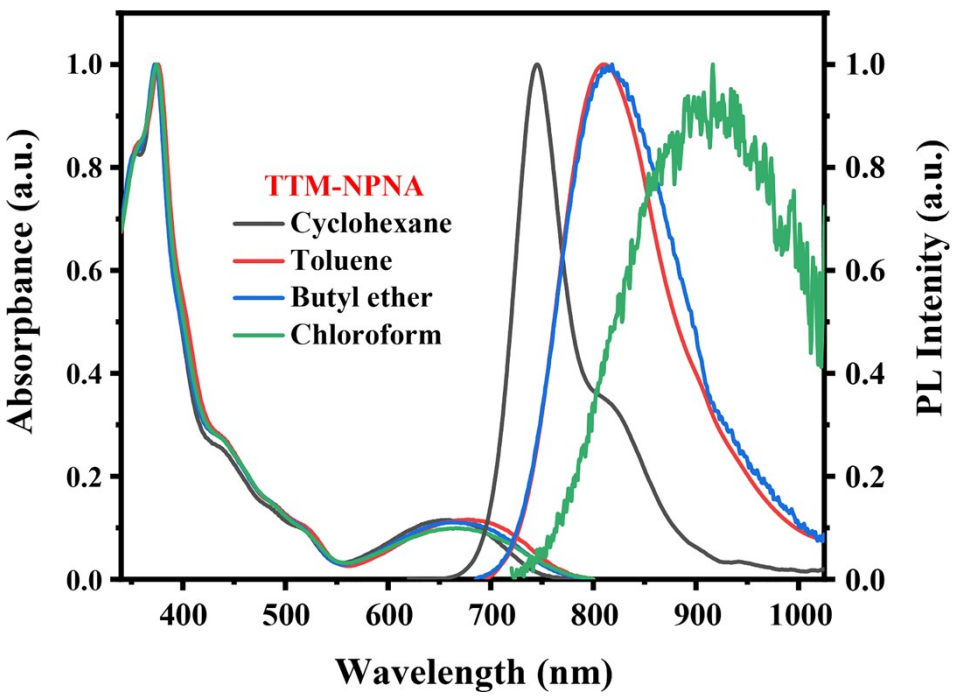

Fig. S6 The normalized UV-vis absorption and PL spectra of **TTM-NPNA** in various solvents (10^{-5} M) at room temperature.

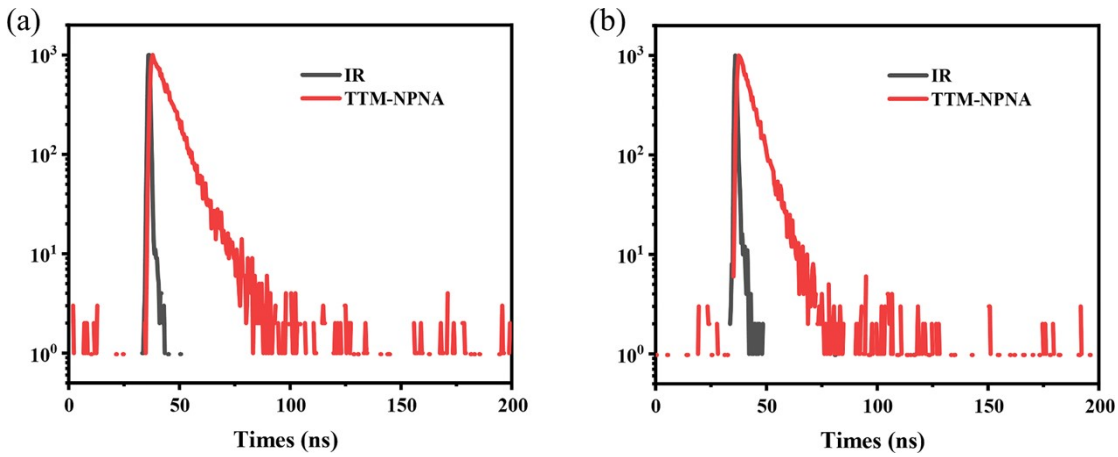

Fig. S7 Fluorescence decay curves of **TTM-NPNA** in (a) toluene and (b) n-butyl ether.

Table S1. Photophysical parameters of **TTM-NPNA** in different solvents.

Radical	Solvent	λ_{abs}[a] (nm)	λ_{PL}[b][c] (nm)	PLQE[b][c] (%)	τ [d] (ns)	k_r^{CT}[e] 10^7 (s^{-1})	k_{nr}^{CT}[e] 10^7 (s^{-1})
TTM-NPNA	cyclohexane	655	745	23	6.7	3.41	11.42
	toluene	671	810	24	7.3	3.27	10.36
	n-butyl ether	665	818	16	5.3	3.01	15.82
	chloroform	669	916	1	-[f]	-	-

[a] long-wavelength absorption in different solvents. [b] excited at 375nm. [c] measured with a calibrated integrating sphere system. [d] measured using Edinburgh fluorescence spectrometer (FLS980) at room temperature. [e] Calculated from the equation: $\phi = k_r/(k_r + k_{nr})$; $\tau = 1/(k_r + k_{nr})$. [f] beyond the measurement-range of the instruments.

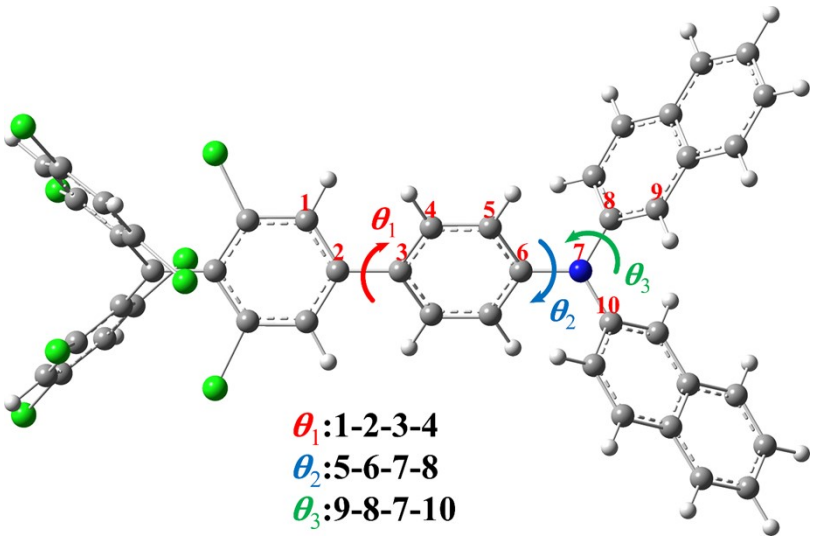

Fig. S8 The optimized geometry configuration of D_0 state and the related dihedral angles (θ_1, θ_2 and θ_3) for **TTM-NPNA** in cyclohexane.

Table S2. The dihedral angle values of θ_1- $\theta_3$and their variations between D_0 and D_1 states.

TTM-NPNA	θ_1 (°)			θ_2 (°)			θ_3 (°)		
	D_0	D_1	Δ_{D1-D0}	D_0	D_1	Δ_{D1-D0}	D_0	D_1	Δ_{D1-D0}
cyclohexane	29.9	35.9	6.0	-34.8	-53.2	-18.4	-44.4	-35.0	9.4
toluene	29.8	35.2	5.4	-34.7	-51.9	-17.2	-44.5	-35.3	9.2
chloroform	29.4	32.6	3.2	-34.2	-47.9	-13.7	-44.9	-36.4	8.5

3. TGA curve and Electrochemical properties

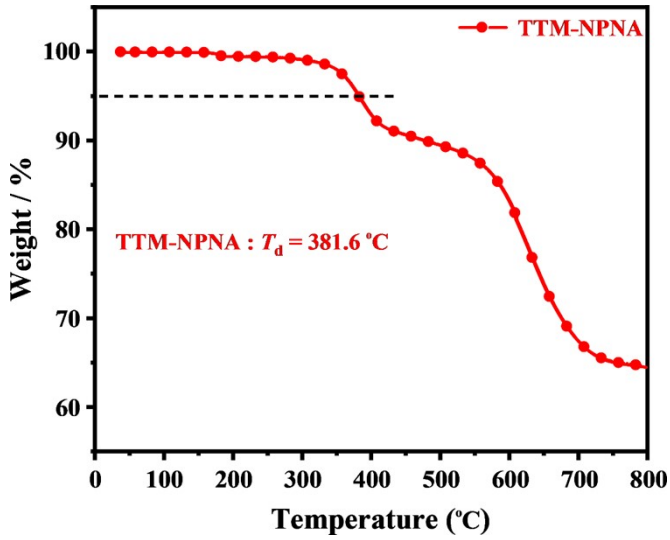

Fig. S9 TGA thermograph of **TTM-NPNA** recorded under nitrogen at a heating rate of 10°C/min.

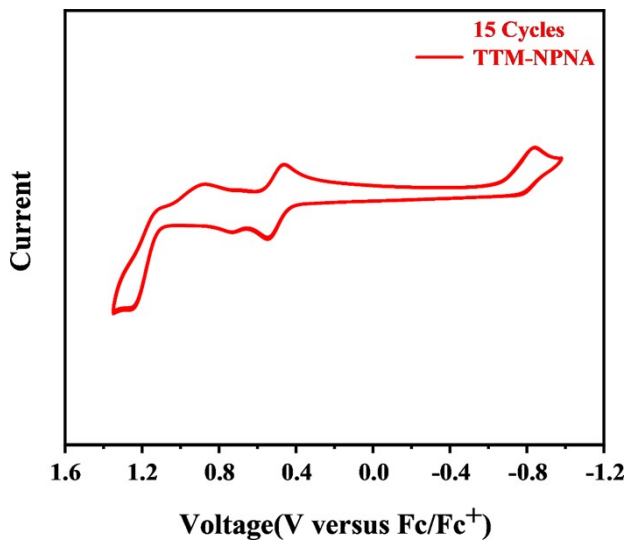

Fig. S10. Repeated cyclic voltammetry measurements (15 cycles) of **TTM-NPNA**.

4. Extracted results of TD-DFT calculations

TTM-NPNA (UB3LYP/6-31G(d,p))

Excitation energies and oscillator strengths:

```
 Excited State   1:   2.091-A        1.5810 eV   784.20 nm   f=0.1332
<S**2>=0.843
      218B ->219B          0.98617
 This state for optimization and/or second-order correction.
 Total Energy, E(TD-HF/TD-KS) =   -5465.52635848
 Copying the excited state density for this state as the 1-particle RhoCI density.

 Excited State   2:   2.305-A        2.4508 eV   505.89 nm   f=0.0056
<S**2>=1.078
      218A ->220A         -0.16112
      219A ->220A          0.29581
      209B ->219B          0.11975
      215B ->219B         -0.44792
      217B ->219B          0.74203
      218B ->219B          0.14752
      218B ->220B         -0.16418

 Excited State   3:   3.438-A        2.4711 eV   501.73 nm   f=0.0000
<S**2>=2.706
      216A ->220A          0.11739
      216A ->224A          0.25205
      217A ->221A         -0.22416
      218A ->221A         -0.22240
      219A ->221A         -0.52468
      219A ->227A         -0.10348
      216B ->219B         -0.16451
      216B ->220B         -0.13409
      216B ->223B         -0.24739
      217B ->221B          0.24547
      218B ->221B          0.54130

 Excited State   4:   3.322-A        2.5607 eV   484.19 nm   f=0.0493
<S**2>=2.509
      216A ->221A         -0.29310
      217A ->224A          0.17737
      218A ->224A          0.14744
      219A ->220A          0.47508
```

219A ->224A 0.27358
219A ->228A 0.10079
216B ->221B 0.29601
217B ->219B -0.30468
217B ->223B -0.19798
218B ->220B -0.40712
218B ->223B -0.26063

Excited State 5: 2.188-A 2.6616 eV 465.82 nm f=0.0090
<S**2>=0.947
218A ->222A -0.23673
219A ->222A 0.14212
210B ->219B 0.14490
212B ->219B 0.44213
213B ->219B 0.54713
214B ->219B -0.51927
216B ->219B -0.26230

Excited State 6: 2.117-A 2.6638 eV 465.44 nm f=0.0018
<S**2>=0.871
212B ->219B 0.11840
213B ->219B 0.14405
214B ->219B -0.15543
216B ->219B 0.94935
218B ->221B 0.11242

Excited State 7: 2.301-A 2.7531 eV 450.34 nm f=0.0195
<S**2>=1.074
216A ->221A -0.11334
218A ->220A 0.25456
219A ->220A -0.17118
219A ->224A 0.14007
209B ->219B -0.24370
211B ->219B -0.19640
215B ->219B 0.57833
216B ->221B 0.11402
217B ->219B 0.57497
218B ->223B -0.12426

Excited State 8: 2.154-A 2.7921 eV 444.05 nm f=0.0075
<S**2>=0.910
218A ->222A -0.21466
219A ->222A 0.14175
210B ->219B 0.16996

212B ->219B 0.70755
213B ->219B -0.38094
214B ->219B 0.44804

Excited State 9: 2.970-A 2.8506 eV 434.93 nm f=0.1757
<S**2>=1.955
215A ->220A 0.10446
216A ->221A 0.24002
217A ->220A -0.16295
217A ->224A -0.15571
218A ->220A -0.12064
219A ->220A 0.48242
219A ->224A -0.20922
219A ->228A 0.12138
209B ->219B -0.18184
211B ->219B -0.35909
215B ->219B 0.34148
215B ->220B -0.11281
216B ->221B -0.23546
217B ->220B 0.17787
217B ->223B 0.14267
218B ->220B -0.13720
218B ->223B 0.24333

Excited State 10: 2.111-A 2.9776 eV 416.39 nm f=0.0038
<S**2>=0.864
218A ->222A -0.11999
218A ->223A 0.14382
210B ->219B 0.90067
212B ->219B -0.31915

Excited State 11: 2.268-A 2.9836 eV 415.56 nm f=0.0115
<S**2>=1.036
218A ->220A 0.13846
218A ->225A 0.10267
209B ->219B -0.41835
211B ->219B 0.81426
218B ->220B -0.12859

Excited State 12: 2.287-A 3.0839 eV 402.04 nm f=0.1136
<S**2>=1.057
212A ->222A 0.13613
218A ->220A -0.14279
218A ->228A 0.14791

218A ->232A -0.12648
219A ->220A 0.24898
206B ->219B 0.12445
207B ->219B 0.45049
209B ->219B 0.48817
211B ->219B 0.26632
212B ->222B -0.10652
215B ->219B 0.40018
217B ->219B 0.11268
218B ->220B 0.13171

Excited State 13: 2.469-A 3.1356 eV 395.41 nm f=0.6507
<S**2>=1.274
216A ->221A -0.10543
218A ->220A -0.30671
218A ->224A 0.11401
219A ->220A 0.35587
207B ->219B -0.21053
209B ->219B -0.30319
216B ->221B 0.12790
217B ->220B -0.11150
218B ->220B 0.69524
218B ->228B -0.12173

Excited State 14: 2.894-A 3.2048 eV 386.87 nm f=0.0217
<S**2>=1.844
216A ->220A 0.11294
216A ->224A 0.21049
217A ->221A -0.31180
219A ->221A 0.76182
219A ->226A 0.10176
219A ->227A -0.16421
216B ->223B -0.19787
217B ->221B 0.25372
218B ->221B 0.14646

Excited State 15: 2.731-A 3.2572 eV 380.65 nm f=0.0279
<S**2>=1.614
216A ->224A -0.16668
217A ->221A 0.20422
219A ->221A 0.24924
216B ->220B 0.11243
216B ->223B 0.17949
217B ->221B -0.27815

218B ->221B 0.78069
218B ->226B 0.13456
218B ->227B 0.10227

Excited State 16: 2.236-A 3.2636 eV 379.90 nm f=0.1915
<S**2>=1.000
218A ->222A -0.54070
219A ->222A 0.61709
210B ->219B -0.27206
212B ->219B -0.35738
213B ->219B -0.12547
218B ->221B 0.11944

Excited State 17: 2.096-A 3.2993 eV 375.79 nm f=0.0007
<S**2>=0.849
208B ->219B -0.23315
213B ->219B 0.67844
214B ->219B 0.67843

Excited State 18: 2.532-A 3.3728 eV 367.60 nm f=0.0338
<S**2>=1.353
216A ->221A 0.16670
217A ->224A -0.12189
218A ->220A 0.62369
219A ->220A 0.33763
219A ->224A 0.33325
215B ->219B -0.22610
216B ->221B -0.13436
217B ->223B 0.15872
218B ->220B 0.32236
218B ->223B -0.10950

Excited State 19: 3.223-A 3.4075 eV 363.86 nm f=0.0011
<S**2>=2.347
214A ->221A 0.11050
216A ->221A 0.20603
217A ->224A -0.22973
218A ->220A -0.38489
218A ->224A 0.10066
219A ->220A -0.10652
219A ->224A 0.51359
219A ->228A -0.15923
216B ->221B -0.20786
217B ->223B 0.19834

218B ->220B -0.16868
218B ->223B -0.43265
218B ->228B -0.10084

Excited State 20: 2.383-A 3.4570 eV 358.64 nm f=0.0087
<S**2>=1.169
218A ->223A -0.56986
219A ->223A 0.72656
219A ->226A -0.19102
210B ->219B 0.15469
218B ->226B 0.11843

5.Electroluminescence Performances

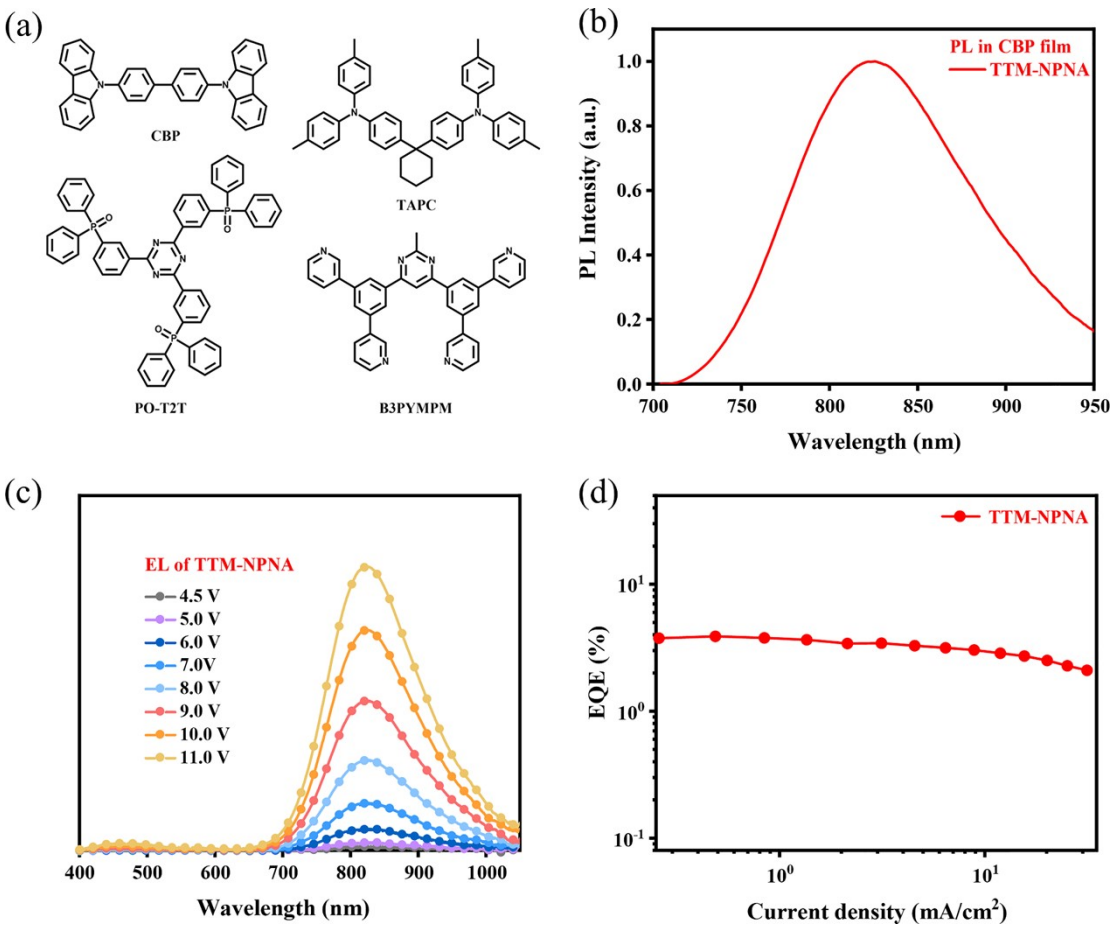

Fig. S11 Electroluminescent properties of **TTM-NPNA**. (a) Materials used in this work; (b) PL spectrum of the **TTM-NPNA** doped film (5.0 wt%-doped in CBP film); (c) EL spectra of **TTM- NPNA** from 4.5-11V; (d) The curve of current density versus EQE for **TTM-NPNA** based device.

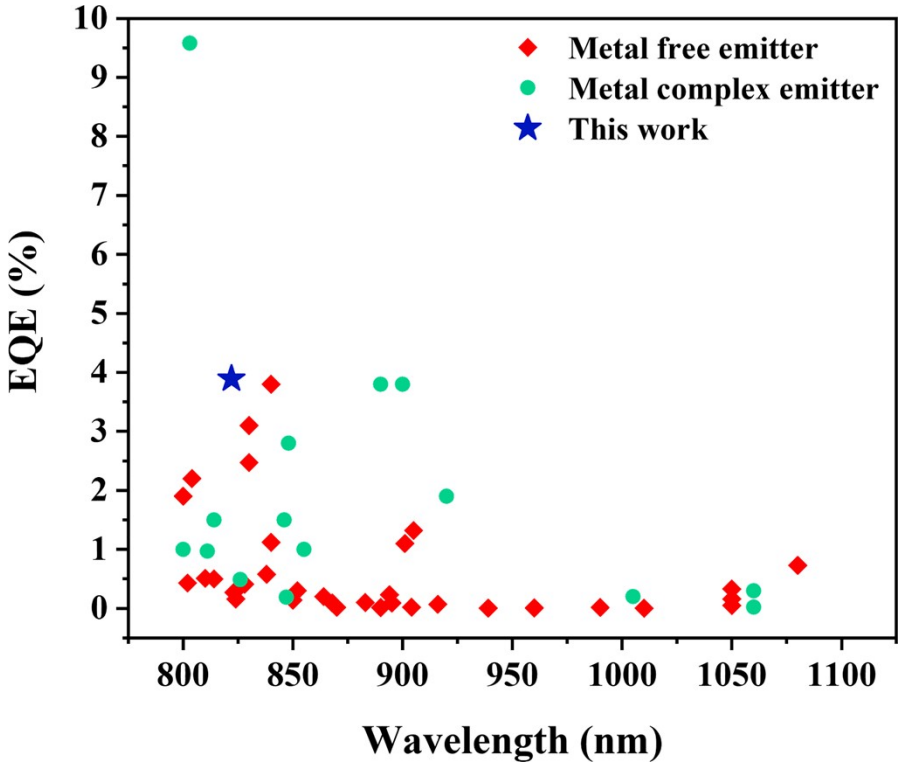

Fig. S12 Summary of EQE in state-of-the-art NIR-OLEDs against the EL peak wavelength (over 800 nm).

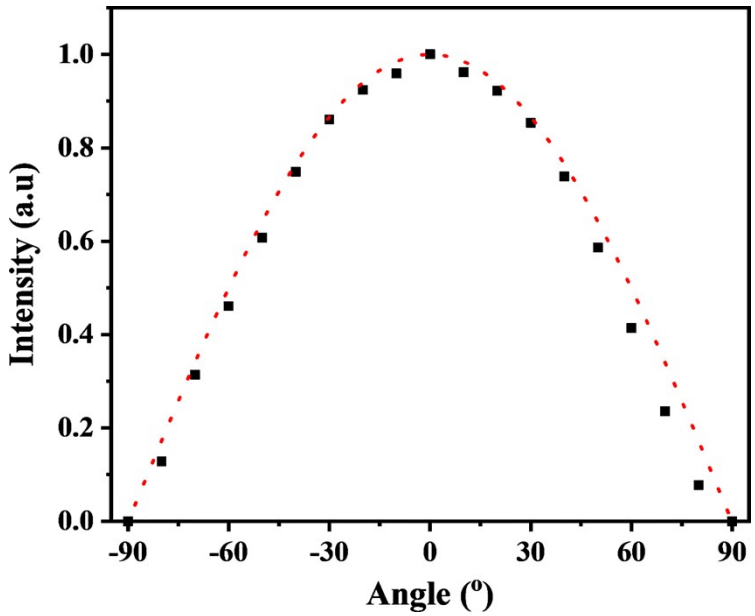

Fig. S13 Measured angular dependence of electroluminescence of **TTM-NPNA** based OLED with the dopant concentration of 5 wt% (black squares), and the angular dependence predicted for Lambertian emission (red dotted line).

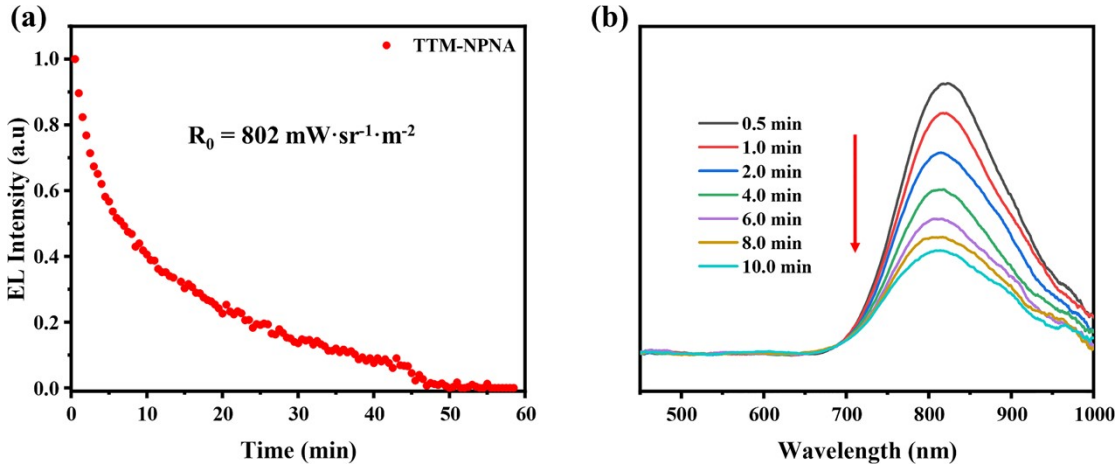

Fig. S14 Variation of (a) EL intensity and (b) spectra of the **TTM-NPNA** based device versus operating time driven at a constant current density of 6 mA/cm^2.

Table S3. Summary of the device performances of NIR-OLEDs published to date with maximum electroluminescent (EL) wavelength over 800 nm.

λ_{ELmax} (nm)	EQE (%)	Emitter material	[ref]	λ_{ELmax} (nm)	EQE (%)	Emitter material	[ref]
800	1.9	metal free emitter	2	800	1	metal complex emitter	3
802	0.43	metal free emitter	4	803	9.58	metal complex emitter	5
804	2.2	metal free emitter	6	811	0.97	metal complex emitter	7
810	0.51	metal free emitter	8	814	1.5	metal complex emitter	9
814	0.5	metal free emitter	10	826	0.49	metal complex emitter	11
822	3.9	metal free emitter	**This work**	847	0.19	metal complex emitter	13
823	0.27	metal free emitter	12	848	2.8	metal complex emitter	15
824	0.16	metal free emitter	14	846	1.5	metal complex emitter	15
828	0.41	metal free emitter	8	855	1	metal complex emitter	17
830	2.47	metal free emitter	16	890	3.8	metal complex emitter	18
830	3.1	metal free emitter	35	900	3.8	metal complex emitter	20
838	0.58	metal free emitter	19	920	1.9	metal complex emitter	22
840	1.12	metal free emitter	21	1005	0.2	metal complex emitter	20
840	3.8	metal free emitter	23	1060	0.022	metal complex emitter	24
850	0.14	metal free emitter	12	1060	0.3	metal complex emitter	25
852	0.3	metal free emitter	8				
864	0.2	metal free emitter	4				
868	0.09	metal free emitter	12				
870	0.02	metal free emitter	12				
883	0.1	metal free emitter	26				

890	0.015	metal free emitter	27
894	0.23	metal free emitter	8
895	0.091	metal free emitter	28
901	1.1	metal free emitter	29
904	0.019	metal free emitter	30
905	1.32	metal free emitter	31
916	0.07	metal free emitter	19
939	0.006	metal free emitter	28
960	0.009	metal free emitter	26
990	0.018	metal free emitter	28
1010	0.003	metal free emitter	32
1050	0.05	metal free emitter	33
1050	0.16	metal free emitter	34
1050	0.33	metal free emitter	34
1080	0.73	metal free emitter	34

6. References

1. Q. Peng, A. Obolda, M. Zhang and F. Li, *Angew. Chem. Int. Ed.*, 2015, **54**, 7091-7095.
2. M. T. Sharbati, F. Panahi, A. Shourvarzi, S. Khademi and F. Emami, *Optik*, 2013, **124**, 52-54.
3. F. Nisic, A. Colombo, C. Dragonetti, D. Roberto, A. Valore, J. M. Malicka, M. Cocchi, G. R. Freeman and J. A. G. Williams, *J. Mater. Chem. C*, 2014, **2**, 1791-1800.
4. X. Du, J. Qi, Z. Zhang, D. Ma and Z. Y. Wang, *Chem. Mater.*, 2012, **24**, 2178-2185.
5. S. F. Wang, Y. Yuan, Y. C. Wei, W. H. Chan, L. W. Fu, B. K. Su, I. Y. Chen, K. J. Chou, P. T. Chen, H. F. Hsu, C. L. Ko, W. Y. Hung, C. S. Lee, P. T. Chou and Y. Chi, *Adv. Funct. Mater.*,2020, **30**, 2002173.
6. Y. Yu, H. Xing, D. Liu, M. Zhao, H. H. Sung, I. D. Williams, J. W. Y. Lam, G. Xie, Z. Zhao and B. Z. Tang, *Angew. Chem. Int. Ed.*, 2022, **61**, e202204279.
7. Z. L. Zhu, S. F. Wang, L. W. Fu, J. H. Tan, C. Cao, Y. Yuan, S. M. Yiu, Y. X. Zhang, Y. Chi and C. S. Lee, *Chem. Eur. J.*, 2022, **28**, e202103202.
8. J.-F. Cheng, Z.-H. Pan, K. Zhang, Y. Zhao, C.-K. Wang, L. Ding, M.-K. Fung and J. Fan, *Chem. Eng. J.*, 2022, **430**, 132744.
9. T.-C. Lee, J.-Y. Hung, Y. Chi, Y.-M. Cheng, G.-H. Lee, P.-T. Chou, C.-C. Chen, C.-H. Chang and C.-C.Wu, *Adv. Funct. Mater.*, 2009, **19**, 2639-2647.

10. Y. Yang, R. T. Farley, T. T. Steckler, S.-H. Eom, J. R. Reynolds, K. S. Schanze and J. Xue, *Appl. Phys. Lett.*, 2008, **93**, 163305.

11. Y. Zhang, Z. Chen, X. Wang, J. He, J. Wu, H. Liu, J. Song, J. Qu, W. T. Chan and W. Y. Wong, *Inorg. Chem.*, 2018, **57**, 14208-14217.

12. G. Qian, Z. Zhong, M. Luo, D. Yu, Z. Zhang, D. Ma, and Y. Wang, *J. Phys. Chem. C*, 2009, **113**, 1589–1595.

13. Y. Zhang, Q. Li, M. Cai, J. Xue and J. Qiao, *J. Mater. Chem. C*, 2020, **8**, 8484-8492.

14. X.-Q. Wang, Y. Hu, Y.-J. Yu, Q.-S. Tian, W.-S. Shen, W.-Y. Yang, Z.-Q. Jiang and L.-S. Liao, *J. Phys. Chem. Lett.*, 2021, **12**, 6034-6040.

15. L. Huang, C. D. Park, T. Fleetham and J. Li, *Appl. Phys. Lett.*, 2016, **109**. 233302.

16. L. Tejerina, A. G. Rapidis, M. Rickhaus, P. Murto, Z. Genene, E. Wang, A. Minotto, H. L. Anderson and F. Cacialli, *J. Mater. Chem. C*, 2022, **10**, 5929-5933.

17. E. Rossi, A. Colombo, C. Dragonetti, D. Roberto, F. Demartin, M. Cocchi, P. Brulatti, V. Fattori and J. A. Williams, *Chem. Commun.*, 2012, **48**, 3182-3184.

18. J. R. Sommer, R. T. Farley, K. R. Graham, Y. Yang, J. R. Reynolds, J. Xue and K. S. Schanze, *ACS Appl. Mater. Interfaces.*, 2009, **1**, 274-278.

19. Y. J. Yu, Y. Hu, S. Y. Yang, W. Luo, Y. Yuan, C. C. Peng, J. F. Liu, A. Khan, Z. Q. Jiang and L. S. Liao, *Angew. Chem. Int. Ed.*, 2020, **59**, 21578-21584.

20. K. R. Graham, Y. Yang, J. R. Sommer, A. H. Shelton, K. S. Schanze, J. Xue and J. R. Reynolds, *Chem. Mater.*, 2011, **23**, 5305-5312.

21. A. Minotto, P. Murto, Z. Genene, A. Zampetti, G. Carnicella, W. Mammo, M. R. Andersson, E. Wang and F. Cacialli, *Adv. Mater*, 2018, **30**, 1706584.

22. L. Cao, J. Li, Z.-Q. Zhu, L. Huang and J. Li, *ACS Appl. Mater. Interfaces.*, 2021, **13**, 60261-60268.

23. A. Shahalizad, A. Malinge, L. Hu, G. Laflamme, L. Haeberlé, D. M. Myers, J. Mao, W. G. Skene and S. Kéna-Cohen, *Adv. Funct. Mater.*, 2021, **31**, 2007119.

24. A. Shahalizad, A. D'Aléo, C. Andraud, M. H. Sazzad, D.-H. Kim, Y. Tsuchiya, J.-C. Ribierre, J.-M. Nunzi and C. Adachi, *Org. Electron.*, 2017, **44**, 50-58.

25. Z.-Q. Chen, F. Ding, Z.-Q. Bian and C.-H. Huang, *Org. Electron.*, 2010, **11**, 369–376.

26. O. Fenwick, J. K. Sprafke, J. Binas, D. V. Kondratuk, F. Di Stasio, H. L. Anderson and

F. Cacialli, *Nano. Lett.*, 2011, **11**, 2451-2456.

27. Y. Xuan, G. Qian, Z. Wang and D. Ma, *Thin Solid Films*, 2008, **516**, 7891-7893.

28. G. Tregnago, T. T. Steckler, O. Fenwick, M. R. Andersson and F. Cacialli, *J. Mater. Chem. C*, 2015, **3**, 2792-2797.

29. U. Balijapalli, R. Nagata, N. Yamada, H. Nakanotani, M. Tanaka, A. D'Aleo, V. Placide, M. Mamada, Y. Tsuchiya and C. Adachi, *Angew. Chem. Int. Ed.*, 2021, **60**, 8477-8482.

30. D. G. Congrave, B. H. Drummond, P. J. Conaghan, H. Francis, S. T. E. Jones, C. P. Grey, N. C. Greenham, D. Credgington and H. Bronstein, *J. Am. Chem. Soc.*, 2019, **141**, 18390-18394.

31. M. T. Sharbati, F. Panahi and A. Gharavi, *IEEE Photon. Technol. Lett.*, 2010, **22**, 1695-1697.

32. Q. Liang, J. Xu, J. Xue and J. Qiao, *Chem. Commun*, 2020, **56**, 8988-8991.

33. G. Qian, B. Dai, M. Luo, D. Yu, J. Zhan, Z. Zhang, D. Ma, and Z. Wang, *Chem. Mater.*, 2008, **20**, 6208–6216.

34. G. Qian, Z. Zhong, M. Luo, D. Yu, Z. Zhang, Z. Y. Wang and D. Ma, *Adv. Mater.*, 2009, **21**, 111-116.

35. J. Ding, S. Dong, M. Zhang and F. Li, *J. Mater. Chem. C*, 2022, **10**, 14116-14121.